Advances in Science and Technology Research Journal

Advances in Science and Technology Research Journal, 18(6), 476–483
https://doi.org/10.12913/22998624/192490
ISSN 2299-8624, License CC-BY 4.0

Received: 2024.07.02
Accepted: 2024.08.20
Published: 2024.09.08

Electrochemical Process Investigation of Synthesizing Magnesium Oxide from Bittern Solution for Solid Oxide Fuel Cells Sealant

Sulistyo[1*], Slamet Saefudin[2], Sulardjaka[1], Reza Abdu Rahman[1,3]

[1] Department of Mechanical Engineering, Universitas Diponegoro, Semarang 50275, Indonesia
[2] Department of Mechanical Engineering, Universitas Muhammadiyah Semarang, Semarang 50275, Indonesia
[3] Department of Mechanical Engineering, Faculty of Engineering, Universitas Pancasila, DKI Jakarta 12640, Indonesia
* Corresponding author's e-mail: sulistyo@lecturer.undip.ac.id

ABSTRACT

Magnesium oxide (MgO) is an essential material for producing solid oxide fuel cells (SOFC) sealant. It can be derived from bittern waste. The common approach uses membrane electrolysis, which requires complex equipment and high energy costs. Alternatively, direct electrolysis can be taken using proper parameters to maximize the production rate. This work analyzes the process according to the input voltage, which varies between 10 and 16 V. The designed working voltage is suitable for direct conversion from renewable sources such as photovoltaic. The evaluation shows that the working voltage notably affects the reaction rate of the bittern solution. The working voltage of 16 V has the lowest power factor (2.58), while the working voltage of 10 V indicates the highest power factor of 3.56. It makes the reaction rate for the working voltage of 10 V extremely low, causing the lowest production rate of MgO with only 4.27 g. Oppositely, the suitable working voltage improves the production of MgO up to 75%. Microscope evaluation indicates that the produced MgO from the process has a lower agglomeration concentration after heat treatment at 700 °C, which is desirable to ensure effective fuel transfer in fuel cell apparatus.

Keywords: brine, bittern, electrolysis, magnesium hydroxide, photoelectric

INTRODUCTION

Seawater is processed through desalination to produce fresh water. The process is vital for regions with limited water supply. Desalination consumes energy, which can be supplied from conventional power plants and other alternative sources. The recent trend indicates that the desalination process can be performed using solar power to reduce the pollution of the conventional model. Solar energy is harvested using photovoltaic [1] or concentrated thermal [2], which can be used as the energy source for desalination. Moreover, the system is possible to operate continuously with the help of an energy storage system [3–5]. However, one crucial problem still occurs in the desalination process, which is related to the waste produced (bittern). The typical process for handling bittern is directly discharged into the open sea. It causes severe damage to the environment due to the high salinity of the solution.

The bittern solution is high in sodium and magnesium content. The two materials are essential for the modern era, such as natrium-based energy storage [6], magnesium hydride for hydrogen storage [7] and magnesium oxide for solid oxide fuel cell (SOFC) sealant [8]. In case of SOFC sealant, magnesium is considered an ideal candidate considering its vast availability and technical suitability, such as density, conductivity and redox stability [9–11]. Also, global society focuses on alternative mining techniques with minimum environmental impact, particularly for magnesium [12]. Thus, reprocessing bittern waste is ideal for reducing the potential impact of the waste [13].

The high magnesium content in bittern solution is generally processed through a membrane electrolysis process [14]. The process involves several steps, using electricity as the main power source for separation [15]. Despite its effectiveness, membrane electrolysis requires complex equipment and high energy costs. Thus, it mostly applies to producing high-economy metals such as lithium [16]. Another process uses a chemical reaction to recover magnesium from the bittern solution [17]. The process is relatively fast and reliable but incurs extra costs regarding the additional reactant. Alternatively, direct electrolysis can be used to extract magnesium from bittern solution [18]. The process is simpler than membrane electrolysis and still in developing phase to improve its performance as a separation technique in the metal production process.

Direct electrolysis operates based on an electrochemical separation technique. The key benefits of the process are design simplification, high production rates, and low environmental impact [19]. Moreover, the method is relatively flexible since the initial results of the process produce magnesium hydroxide ($Mg(OH)_2$), which is useful for various applications. For example, Amrulloh et al. [20] utilized $Mg(OH)_2$ from bittern solution for Pb and Cd separation processes, showing a good kinetic rate of the process using nanostructured $Mg(OH)_2$. Further modification is performed by doping the produced magnesium with zinc oxide to produce hydrogen from wastewater recovery [21]. Thus, reprocessing bittern solution is considerably effective in supporting magnesium's usability in the modern era.

Optimization is performed to ensure the effective direct electrolysis for bittern solution. Guo et al. [22] employed liquid metal to accelerate the reaction rate, resulting in a lower carbon emission of the process with only 20.6 kg of CO_2/kg Mg. Choi et al. [23] took a different process indicator, which investigated an energy-based model of combined electrolysis and carbonation, indicating that 91.3% of CO_2 could be recovered from the process using the final products $CaCO_3$ and $MgCO_3$. The key aspect of the direct electrolysis is the reaction mechanism of the solution. Cai et al. [24] examined the mechanism of magnesium ion release at the magnesium anode, demonstrating the direct relation between the applied electricity and the kinetic rate of reaction. Technical aspects such as sediment formation, power factor, and solution composition are crucial to ensure effective direct electrolysis [25]. Thus, the operational consideration and composition of the bittern solution are critical aspects that affect the quality of the reaction process.

The basic concept of electrolysis is related to ion exchange, causing variations in pH level, temperature, and chemical composition of the solution throughout the process. For example, the study performed by Li et al. [26] showed the relation between the working voltage and boiling rate of the electrolysis process. Another study focused on the variation of working voltage (2 and 3 V) for the process, showing a direct impact on the kinetic rate and changes in the solution during the process [27]. Different work focuses on numerical modelling for optimizing the technical parameters of the electrolysis process. The work here [28] analyzed numerically the critical aspect of direct electrolysis, confirming that the working voltage and current density are the major factors which significantly affect the quality of the process. A successful improvement in optimizing electrolysis for hydrogen production leads to a significant achievement in this system [29]. The same consideration is important for optimizing the electrolysis process for magnesium production, particularly from waste sources, to support the development of recycling and green mining processes.

Limited work focuses on the experimental evaluation of the operational parameter and the quality of the produced magnesium from the bittern solution. Therefore, the present study aims to experimentally investigate the effect of the parameter process on the direct electrolysis of bittern solution for producing magnesium. The study focuses on the operational aspect that can be supported by renewable sources, such as photovoltaic, to drive the electrolysis process [30]. The detailed analysis of the process and characterization of the produced magnesium are expected to bring positive contributions to the development of the green electrolysis process, reducing the risk of pollution caused by bittern solution and maximizing the potential of renewable sources to support the green mining process for extracting magnesium from alternative source.

MATERIALS AND METHOD

This work used a direct electrolysis reactor consisting of electrodes, bittern solution, distilled water, and a power source (Figure 1a). The

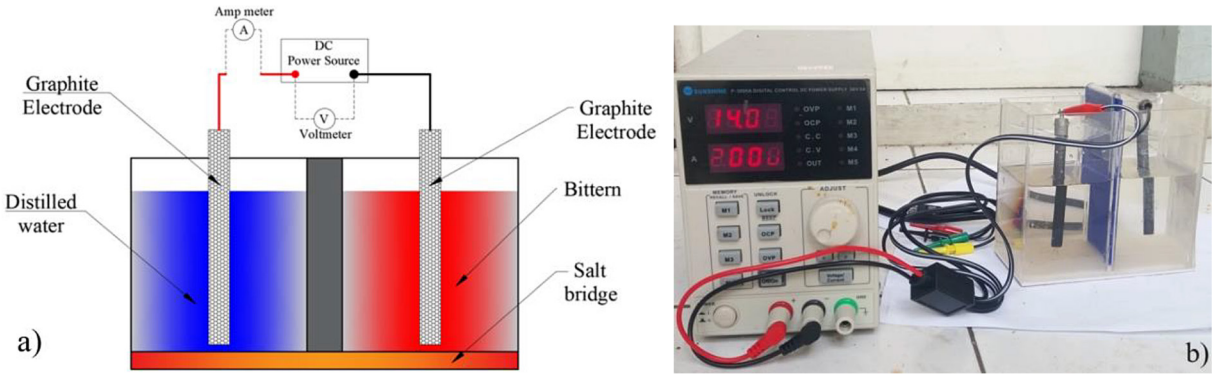

Figure 1. Schematic design for the electrolysis process using graphite electrodes

proposed model has one major benefit regarding the simplicity of the apparatus and process control as discussed in this work [31]. Graphite was used as an electrode since it has good electrical conductivity and corrosion resistance to the high concentration of salt water [32]. Figure 1b shows the photograph of the experimental process. The compartment was made of acrylic (thickness 2 mm) with net volume of 200 ml for each compartment. The bittern solution was located in the negative compartment (cathode), while the distilled water was in the positive compartment (anode). A salt bridge was prepared at the bottom of the compartment to ensure the continuity of the electrolysis process.

The bittern solution was obtained from local salt producer. The solution was filtered several times to remove the impurities. The bittern was characterized using XRF (X-ray fluorescence) to provide a detailed basis. The major contents from the solution were Na (6.4284%), Mg (2.2759%), Cl (11.646%), K (0.3168%), and Ca (0.4457%). Then, the electrolysis was performed. The applied current from the power source was limited to 2 A throughout the process, while the working voltage was set between 10 to 16 V (interval 2 V). The electrolysis changes the current and voltage from power source to the reactor [33]. Thus, both values were measured simultaneously to determine the power factor and voltage drop. The temperature, pH, and total dissolved solids (TDS) were measured every fifteen minutes. The total duration of the process was two hours.

RESULTS AND DISCUSSION

The magnesium hydroxide obtained from the process is used as the initial evaluation. As seen in Figure 2, there is a positive trend in

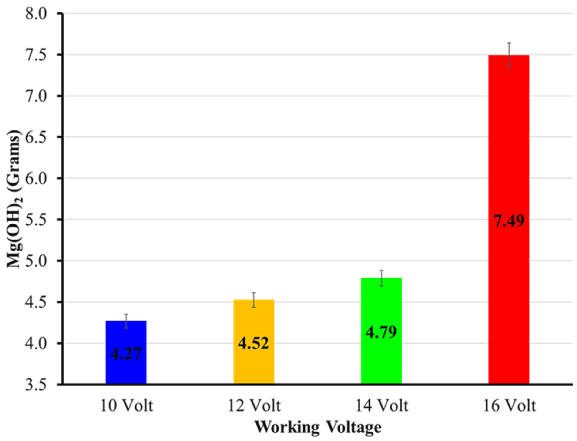

Figure 2. Voltage impact on the synthesis capability of magnesium hydroxide

the increment of working voltage and the produced magnesium hydroxide. The value varies between 5.97% and 12.16% under the designed working voltage of 10–16 V. Interestingly, the produced magnesium hydroxide increases less than 10% between 12 and 14 V. However, it improves significantly using 16 V, where the magnesium hydroxide produced increases by around 65.9%. Since the process was taken using the same current, it confirms that working voltage is the most crucial factor that drives the reaction rate throughout the process [34].

The detailed profile of the process is plotted in Figure 3, which presents the power factor and voltage drop. The power factor increases at the initial process (Figure 3a). However, the profile decreases after a certain time, representing the kinetic reaction changes. The working voltage of 10 V is the only model that shows a continuous increment, indicating a slow reaction rate causing the lowest production rate (Figure 2). Figure 3b plots the voltage drop for each working voltage,

corresponding to the decrement in power factor. The highest voltage drop occurs with the working voltage of 16 V, confirming the effective process of ion exchanges during the electrolysis. It also indicates that the higher voltage leads to a substantial reaction time, increasing the production rate of magnesium hydroxide.

Electrolysis is an endothermic process [35] we demonstrate the full abatement of Mg^{2+}, with concomitant recovery of magnesium hydroxide. We have studied the influence of three operational variables, current density, temperature and forced mass transport in the coulombic efficiency, cell voltage between the electrodes, solid purity and lithium ions loss. Response surface methodology was used to model the system. Our results show that both in terms of energy efficiency, product purity and minimal Li^+ loss it is best to work at very low current density, high flow rate, and high temperature (32 $A \cdot m^{-2}$, 60 °C, and 18 $L \cdot h^{-1}$, resulting in temperature increment within the compartment. The initial temperature for each compartment was 30 °C (± 0.5 °C). The temperature of the anode compartment (Figure 4a) increases steadily for the working voltage between 10 and 14 V, especially after reaching 50 °C. The high kinetic reaction with 16 V causes the maximum temperature at 56.6 °C. It supports the justification of a higher kinetic rate as presented in the power factor and voltage drop (Figure 3) for the same voltage. Also, the reaction occurs in the cathode at a higher rate, making the temperature at this compartment higher (Figure 4b). One crucial factor relates to the composition of the bittern, which probably leads to a faster temperature distribution within the compartment. As a result, the final temperature is relatively similar, particularly between 14 and 16 V. Compared to the produced magnesium hydroxide (Figure 2), it is clear that the temperature increment is not proportional to the reaction process of the bittern solution. Thus, choosing a suitable working voltage becomes crucial to maintaining the effective reaction rate during the process.

The effect of the reaction process changes the pH value for each compartment. As shown in Figure

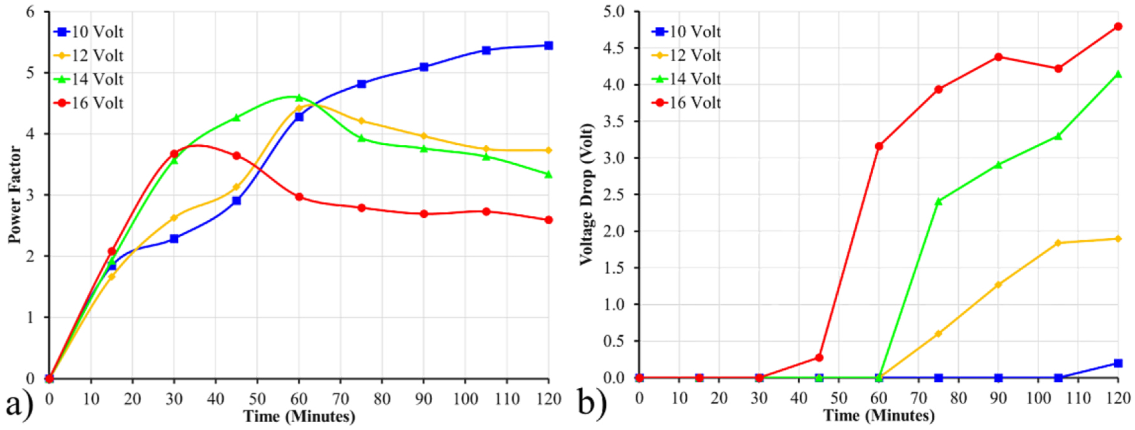

Figure 3. The power factor (a) and voltage drop (b) profile from the electrolysis process

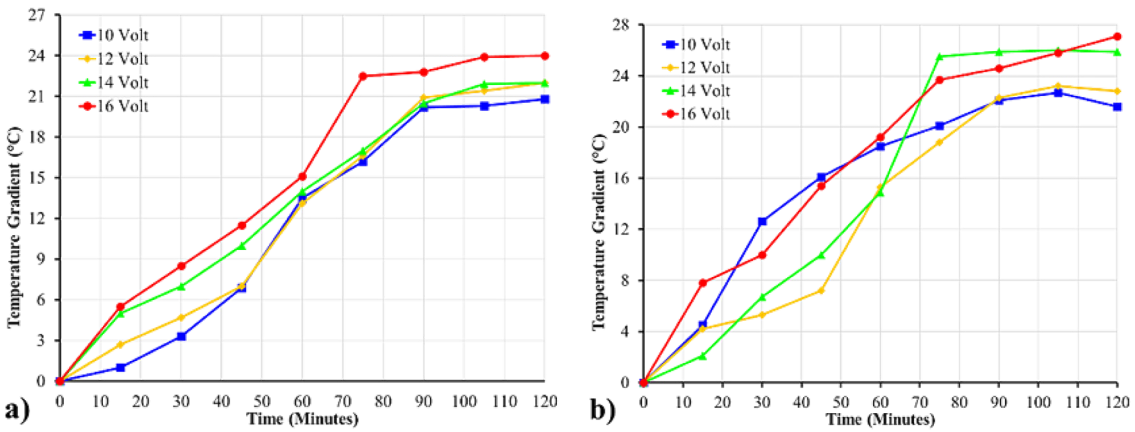

Figure 4. Temperature changes during the electrolysis process on the anode (a) and cathode (b) sides

5, each compartment shows the opposite characteristic of the pH value. The pH value for the anode compartment increases due to formation of magnesium hydroxide (Figure 5a). The slow reaction rate for a working voltage of 10 V makes the pH value increase by 3.8×10^{-2}/minute. It confirms the lowest formation of magnesium hydroxide based on this parameter. Interestingly, the decrement in pH level on the cathode side tends to be faster at the beginning of the reaction (Figure 5b). It indicates that the solution becomes acidic, particularly for the first period of the reaction process (15 minutes). The value ranges between 2.5 and 2.66, which can be observed for all working voltages.

The opposite pH value profile is shown for each compartment according to the total dissolved solids (TDS, Figure 6). The low content of TDS for the anode side (Figure 6a) is affected by the reaction process, which occurs mainly on the cathode side. It confirms the temperature profile for the anode side, which is steadily increased compared to the cathode side (Figure 4a). Since the rate of change of TDS and the reaction rate are closely correlated, it is evident that the voltage of 10 V has the slowest rate of reduction (16.1 ppm/minute). However, significant variation is observed for the higher voltage. For example, the working voltage of 14 V experiences fluctuation, while the working voltage of 12 and 16 V show a steady decrement. The cathode side experienced an increase in TDS due to the formation of magnesium hydroxide on the electrode side (Figure 6b), confirming the decrement in pH value (Figure 5b). The stable value over 4×10^3 ppm is achieved after 45 minutes with a working voltage of 16 V. The low reaction rate of the working voltage of 10 V causes a slower TDS increment. In addition, the final TDS value ranges between 4.633 to 4.734×10^3 ppm, showing that the electrolysis process for the bittern solution can be performed with the given working voltage.

The electrolyte from the electrolysis process was processed for heat treatment. The aim was to observe the microstructure and crystal profile to examine the quality of the produced magnesium oxide. The first heat treatment was performed at a temperature of 110 °C to eliminate impurities.

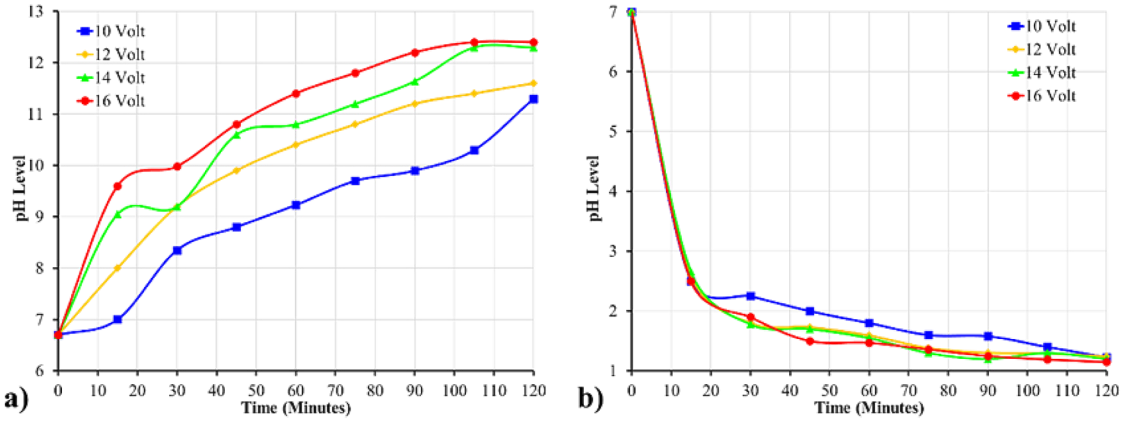

Figure 5. pH variations on the anode (a) and cathode (b) sides during the electrolysis process

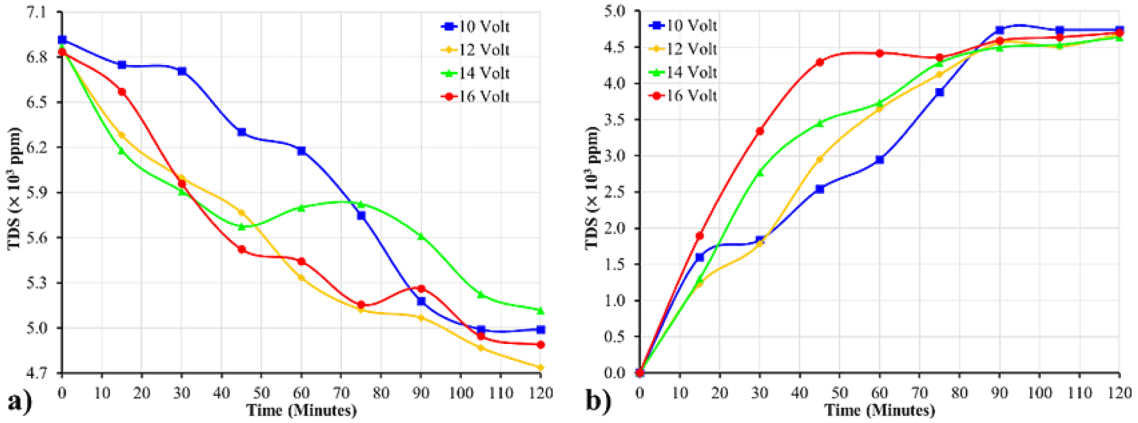

Figure 6. TDS value variations on the anode (a) and cathode (b) sides during the electrolysis process

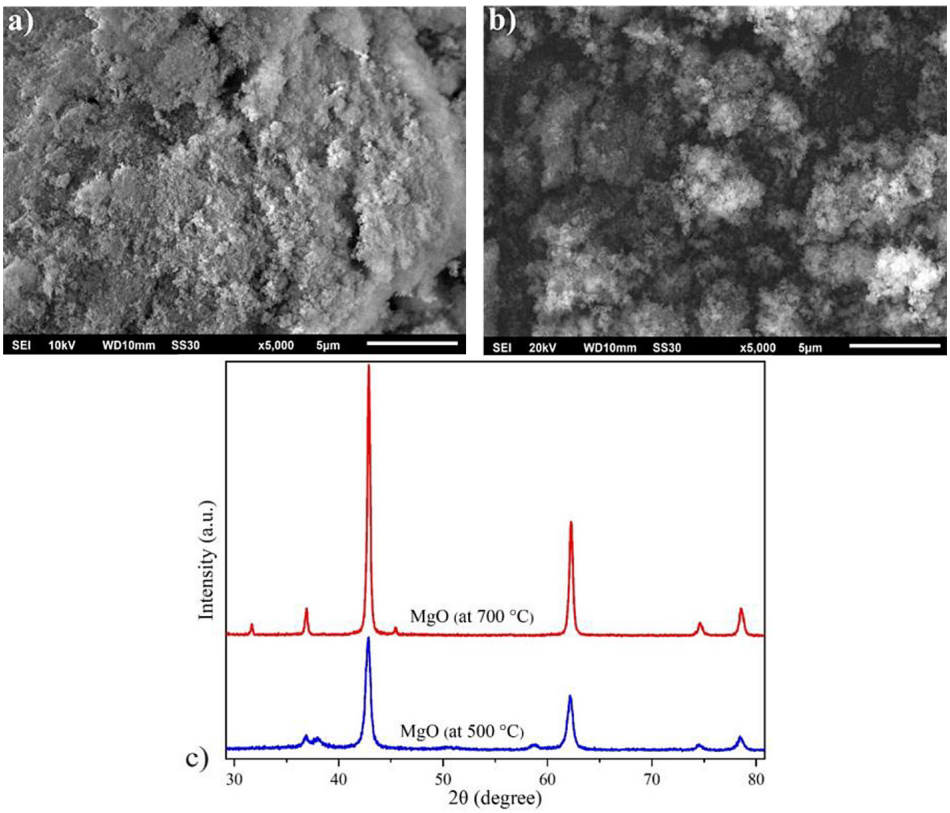

Figure 7. Scanning electron microscope (SEM) for MgO after heat treatment at 500 °C (a) and 700 °C (b), and (c) its X-ray diffractometer (XRD) pattern

Then, the remaining powder was heated at temperatures 500 °C and 700 °C. The temperature represents the working temperature of low and medium temperature SOFC [36].

The SEM profile for the heated magnesium oxide at 500 °C shows large clumps (Figure 7a). It is commonly affected by the agglomeration process of magnesium oxide. In contrast, the treated magnesium oxide at 700 °C indicates a lower concentration of agglomerated profile (Figure 7b). During the heat treatment, the mass of the powder was decreased around 0.484 g. Thus, a higher temperature is desirable to minimize the formation of agglomeration within the produced magnesium. A lower agglomeration concentration is advantageous for SOFC since it requires suitable possibility to ensure effective fuel transfer during the operation [37]. The XRD pattern shows the intensity at 2θ of 36.8°, 42.8°, 62.2°, 74.5°, and 78.4° (Figure 7c). Both XRD patterns indicate a lower intense peak compared to its base ($Mg(OH)_2$) [38], showing the suitable quality of the produced magnesium oxide from this work. Thus, the given parameter in this work is feasible to drive the reaction process to harvest magnesium oxide from bittern solution.

CONCLUSIONS

The present study demonstrates that the bittern solution is feasible to be processed through direct electrolysis for magnesium oxide production. The key parameter process is highly related to the working voltage. It shows a significant improvement in the produced magnesium oxide up to 75.45% using a working voltage of 16 V. The lowest power factor of the given voltage indicates the effective reaction rate. This is followed by a high temperature increment in the reactor compartment, including changes in pH and TDS values. The average temperature indicates the variation in each compartment only 2.8 °C and 3.8 °C, showing the given working voltage resulting in different reaction rates of the process. The same phenomenon is also observed for the pH and TDS values.

The morphology of the produced magnesium oxide indicates agglomeration, which can be reduced through heat treatment. The XRD pattern shows a lower number of intensity peaks, indicating the suitable quality of the produced magnesium oxide. The low agglomeration profile is essential to improve the fuel transfer rate for the fuel cell. Thus, the finding from this work is

applicable to producing magnesium oxide from bittern solution. Further evaluation is advisable by examining a large-scale model, including a detailed energy cost and improvement on the heat distribution within the compartment to improve the direct electrolysis process.

REFERENCES

1. Beithou N, Mansour MA, Abdellatif N, Alsaqoor S, Tarawneh S, Jaber AH, Andruszkiewicz A, Alsqour M, Borowski G, Alahmer A, Siderska J. Effect of the Residential Photovoltaic Systems Evolution on Electricity and Thermal Energy Usage in Jordan. Advances in Science and Technology Research Journal 2023; 17(3): 79–87.
2. Suyitno BM, Rahman RA, Sukma H, Rahmalina D. the Assessment of Reflector Material Durability for Concentrated Solar Power Based on Environment Exposure and Accelerated Aging Test. Eastern-European Journal of Enterprise Technologies 2022; 6(12–120):22–9.
3. Tanim TR, Yang Z, Colclasure AM, Chinnam PR, Gasper P, Lin Y, Yu L, Weddle PJ, Wen J, Dufek EJ, Bloom I, Smith K, Dickerson CC, Evans MC, Tsai Y, Dunlop AR, Trask SE, Polzin BJ, Jansen AN. Extended cycle life implications of fast charging for lithium-ion battery cathode. Energy Storage Materials 2021; 41(May): 656–66. https://doi.org/10.1016/j.ensm.2021.07.001
4. Ode L, Firman M, Rahmalina D, Rahman RA. Hybrid energy-temperature method (HETM): A low-cost apparatus and reliable method for estimating the thermal capacity of solid – liquid phase change material for heat storage system. HardwareX 2023; 16(Dec.): e00496.
5. Miao J, Tong Z, Tong S, Zhang J, Mao J. State of charge estimation of lithium-ion battery for electric vehicles under extreme operating temperatures based on an adaptive temporal convolutional network. Batteries 2022; 8(10).
6. Suyitno BM, Anggrainy R, Plamonia N, Rahman RA. Preliminary characterization and thermal evaluation of a direct contact cascaded immiscible inorganic salt/high-density polyethylene as moderate temperature heat storage material. Results in Materials 2023; 19(June): 100443. https://doi.org/10.1016/j.rinma.2023.100443
7. Yao J, Wang B, Chen H, Han Z, Wu Y, Cai Z, Manggada GW, Elsayed MA, Zhou S. Effect of copper cluster on reaction pathways of carbon dioxide hydrogenation on magnesium hydride surface. International Journal of Hydrogen Energy. 2024; 78(April): 1089–98. https://doi.org/10.1016/j.ijhydene.2024.06.382
8. Zheng K, Lach J, Zhao H, Huang X, Qi K. Magnesium-doped Sr2(Fe,Mo)O6−δ double perovskites with excellent redox stability as stable electrode materials for symmetrical solid oxide fuel cells. Membranes 2022; 12(10).
9. Yang Y, Li M, Ren Y, Li Y, Xia C. Magnesium oxide as synergistic catalyst for oxygen reduction reaction on strontium doped lanthanum cobalt ferrite. International Journal of Hydrogen Energy 2018; 43(7): 3797–802. https://doi.org/10.1016/j.ijhydene.2017.12.183
10. Liang Q, Tang P, Zhou J, Bai J, Tian D, Zhu X, Zhou D, Wang N, Yan W. Effect of MgO and Fe2O3 dual sintering aids on the microstructure and electrochemical performance of the solid state Gd0.2Ce0.8O2-δ electrolyte in intermediate-temperature solid oxide fuel cells. Frontiers in Chemistry 2022; 10(Sept.): 1–14.
11. Krainova DA, Saetova NS, Polyakova IG, Farlenkov AS, Zamyatin DA, Kuzmin A V. Behaviour of 54.4SiO2-13.7Na2O-1.7K2O-5.0CaO-12.4MgO-0.6Y2O3-11.3Al2O3-0.9B2O3 HT-SOFC glass sealant under oxidising and reducing atmospheres. Ceramics International 2022; 48(5): 6124–30. https://doi.org/10.1016/j.ceramint.2021.11.151
12. Rodrigues DM, Carvalho AP, do Amaral Fragoso R, Hein T, de Brito AG. Bittern-impregnated sisal: An alternative magnesium source for phosphorus recovery through struvite precipitation? Journal of Water Process Engineering 2022; 50(Oct.).
13. Khajouei G, Park H Il, Finklea HO, Ziemkiewicz PF, Peltier EF, Lin LS. Produced water softening using high-pH catholyte from brine electrolysis: reducing chemical transportation and environmental footprints. Journal of Water Process Engineering 2021; 40(Dec. 2020): 101911.
14. Pan XJ, Dou ZH, Zhang TA, Meng DL, Fan YY. Separation of metal ions and resource utilization of magnesium from saline lake brine by membrane electrolysis. Separation and Purification Technology 2020; 251(June): 117316.
15. Lee Y, Yang JK, Park JH. Thermodynamics of fluoride-based molten fluxes for extraction of magnesium through the low temperature solid oxide membrane (LT-SOM) process. Calphad: Computer Coupling of Phase Diagrams and Thermochemistry 2018; 62(July): 232–7. https://doi.org/10.1016/j.calphad.2018.07.006
16. Díaz Nieto CH, Palacios NA, Verbeeck K, Prévoteau A, Rabaey K, Flexer V. Membrane electrolysis for the removal of Mg^{2+} and Ca^{2+} from lithium rich brines. Water Research 2019; 154: 117–24.
17. Sun B, Li Y, Guo H, Chen X, Cao J. Fast and complete recovery of magnesium from sea bittern to synthesize magnesium hydroxide hexagonal nanosheet for enhanced flame retardancy and mechanical properties of epoxy resin. Desalination

2024; 583(5340): 117716. https://doi.org/10.1016/j.desal.2024.117716

18. Mahmud N, Alvarez DVF, Ibrahim MH, El-Naas MH, Esposito DV. Magnesium recovery from desalination reject brine as pretreatment for membraneless electrolysis. Desalination 2022; 525(Nov): 115489.
19. Ma X, Li M, Feng C, He Z. Electrochemical nitrate removal with simultaneous magnesium recovery from a mimicked RO brine assisted by in situ chloride ions. Journal of Hazardous Materials 2020; 388(Jan.): 122085.
20. Amrulloh H, Kurniawan YS, Ichsan C, Jelita J, Simanjuntak W, Situmeang RTM, Krisbiantoro PA. Highly efficient removal of Pb(II) and Cd(II) ions using magnesium hydroxide nanostructure prepared from seawater bittern by electrochemical method. Colloids and Surfaces A: Physicochemical and Engineering Aspects 2021; 631(Oct.): 127687.
21. Alebrahim MA, Ahmad AA, Alakhras LA, Al-Bataineh QM. Magnesium-doped zinc oxide film for hydrogen production from wastewater. Materials Chemistry and Physics 2024; 320(May): 129440. https://doi.org/10.1016/j.matchemphys.2024.129440
22. Guo L, Yin H, Li W, Wang S, Du K, Shi H, Wang X, Wang D. Liquid-metal-electrode-assisted electrolysis for the production of sodium and magnesium. Journal of Magnesium and Alloys 2024; 1–13. https://doi.org/10.1016/j.jma.2024.01.028
23. Choi WY, Aravena C, Park J, Kang D, Yoo Y. Performance prediction and evaluation of CO_2 utilization with conjoined electrolysis and carbonation using desalinated rejected seawater brine. Desalination 2021; 509(Feb.): 115068.
24. Cai Y, Han Z, Lin X, Du J, Lei Z, Ye Z, Zhu J. Mechanisms of releasing magnesium ions from a magnesium anode in an electrolysis reactor with struvite precipitation. Journal of Environmental Chemical Engineering 2022; 10(1): 106661.
25. Díaz Nieto CH, Mata MA, Palacios CJO, Palacios NA, Torres WR, Vera ML, Flexer V. Transmembrane fluxes during electrolysis in high salinity brines: Effects on lithium and other raw materials recovery. Electrochimica Acta 2023; 454(March): 8–10.
26. Li L, Nakajima H, Moriyama A, Ito K. Theoretical analysis of the effect of boiling on the electrolysis voltage of a polymer electrolyte membrane water electrolyzer (PEMWE). Journal of Power Sources 2023; 575(May).
27. Lalia BS, Khalil A, Hashaikeh R. Selective electrochemical separation and recovery of calcium and magnesium from brine. Separation and Purification Technology 2021; 264(Dec.): 118416.
28. Zhang G, Yan Z, Liu Q, Lu G. Multi-objective optimization strategy for multipolar magnesium electrolysis cell based on thermal-electric model. Chemical Engineering Journal 2024; 490(Jan.): 151690. https://doi.org/10.1016/j.cej.2024.151690
29. Lattieff FA, Majdi HS, Jweeg MJ, Al-Qrimli FAM. Improvements in hydrogen evolution through a new design of coupling inexpensive nanocomposite electrocatalysts driven by high-voltage electrolysis. Chemical Engineering Research and Design 2023; 196: 468–82.
30. Contreras M, Mba-Wright M, Wulf C, Stanier CO, Mubeen S. Technoeconomic analysis of photoelectrochemical hydrogen production from desalination waste brine using concentrated solar flux. International Journal of Hydrogen Energy 2023; 49: 360–72.
31. Kowthaman CN, Senthil Kumar P, Arul Mozhi Selvan V. Micro-patterned graphite electrodes: An analysis and optimization of process parameters on hydrogen evolution in water electrolysis. Fuel 2021; 305(Aug.): 121542. https://doi.org/10.1016/j.fuel.2021.121542
32. Abdollahi Asl M, Tahvildari K, Bigdeli T. Eco-friendly synthesis of biodiesel from WCO by using electrolysis technique with graphite electrodes. Fuel 2020; 270(Jan.): 117582. https://doi.org/10.1016/j.fuel.2020.117582
33. Jang D, Cho HS, Lee S, Park M, Kim S, Park H, Kang S. Investigation of the operation characteristics and optimization of an alkaline water electrolysis system at high temperature and a high current density. Journal of Cleaner Production 2023; 424(Aug.): 138862. https://doi.org/10.1016/j.jclepro.2023.138862
34. Bouazza A, Ait Hak S, Faddouli A, Khaless K, Benhida R. Kainite crystallization from RO bittern: A novel approach using discontinuous evaporation. Desalination 2024; 582(Feb.): 117652. https://doi.org/10.1016/j.desal.2024.117652
35. Díaz Nieto CH, Kortsarz JA, Vera ML, Flexer V. Effect of temperature, current density and mass transport during the electrolytic removal of magnesium ions from lithium rich brines. Desalination 2022; 529(Nov.).
36. Irshad M, Siraj K, Raza R, Ali A, Tiwari P, Zhu B, Rafique A, Ali A, Ullah MK, Usman A. A brief description of high temperature solid oxide fuel cell's operation, materials, design, fabrication technologies and performance. Applied Sciences (Switzerland) 2016; 6(3).
37. Han Z, Dong H, Wang H, Yang Y, Yu H, Yang Z. Temperature-dependent chemical incompatibility between NiO-YSZ anode and alkaline earth metal oxides: Implications for surface decoration of SOFC anode. Journal of Alloys and Compounds 2023; 968(June): 172150.
38. Battaglia G, Ventimiglia L, Vicari F, Tamburini A, Cipollina A, Micale G. Characterization of $Mg(OH)_2$ powders produced from real saltworks bitterns at a pilot scale. Powder Technology 2024; 443(April): 119918. https://doi.org/10.1016/j.powtec.2024.119918